Chronic inflammation partially recapitulates the gene expression signature of aging

Tomer Landsberger[1 #], Ido Amit[1], Uri Alon[2 #]

1. Department of Immunology, Weizmann Institute of Science, Rehovot, Israel
2. Department of Molecular Cell Biology, Weizmann Institute of Science, Rehovot, Israel

Correspondence should be addressed to: tomer.landsberger@gmail.com; uri.alon@weizmann.ac.il

Abstract

Mammalian aging is accompanied by low-grade chronic inflammation (CI), termed *inflammaging*, commonly regarded as a proximal cause of aging-related dysfunction. Inflammaging is thought to lie downstream of core drivers of aging consisting of cellular and molecular changes and damage forms, such as aberrant epigenomes and transcriptomes. Here we test the reverse hypothesis, that CI itself causes multiple aging-related changes at the transcriptional level – and thus that inflammation is a core driver of aging and some of the transcriptional changes are downstream of it. By analyzing bulk and single-cell RNA sequencing data, we find that interventions in lung, liver, and kidney that cause CI in young mice partially recapitulate the gene expression signature of aging mice in the same organs. This recapitulation occurs in most measured cell populations, including parenchymal, immune and stromal cells, and consists of both inflammation signals themselves and non-inflammation related genes. We find that senolytic treatment reverses the shared gene expression component of aging and CI. The results point to the potential role of age-dependent CI as a core driver of aging.

Main

Aging is defined by progressive loss of function and increased vulnerability to illness and death. One of the pervasive features of mammalian aging is a low-grade chronic inflammatory status, termed "inflammaging", occurring in the absence of overt infection [1]. Inflammaging entails high levels of circulating cytokine and pro-inflammatory factors, as well as tissue-localized inflammation. Whereas acute inflammation is crucial to defend against invading pathogens and during tissue trauma, long-term inflammation is often deleterious, associated with increased mortality [2] and with age-correlated pathologies, including cardiovascular disease, cancer, diabetes and atherosclerosis [3].

Several possible sources of inflammaging have been proposed [4], including pro-inflammatory self-debris such as damaged macromolecules and dying cell fractions, free radicals from oxidative stress, and the buildup of senescent cells [5], cells that underwent stress-mediated irreversible cell-cycle arrest and secrete a cocktail of immunostimulatory molecules called senescence-associated secretory profile (SASP). These factors accumulate with age due to

increased production and/or inadequate elimination by diminishingly effective resilience mechanisms (e.g. the immune system) [6].

The proposed etiology of inflammaging thus consists of molecular events which are associated with normal aging. The influential hallmarks of aging [7] paper describes inflammaging as a high-level phenotype of aging which is a net result of more primary causes. While it is widely recognized that inflammaging may constitute a proximal cause of tissue dysfunction and pathology in aging, its potential role in reinforcing lower-level cellular and molecular aging hallmarks is seldom explored. Understanding the causal interconnections of inflammaging with other core changes of aging, e.g., gene expression changes, is crucial in order to realize the potential of inflammaging as a target for treating aging and age-related morbidity.

Here we aim to test a hypothesis that runs counter to the prevailing view that inflammaging lies only downstream of other hallmarks of aging. Instead, we propose that CI drives many age-related molecular changes, including age-related changes in non-immune cells.

To test this hypothesis, we compare the gene expression profile of aging to the gene expression profile of CI in the young. We utilize published datasets of bulk and single-cell RNA sequencing (scRNA-seq) for murine aging and for interventions that induce CI in young animals in three organs - pulmonary fibrosis of the lungs, non-alcoholic steatohepatitis of the liver, and obstructive nephropathy of the kidney. We find that CI sizably recapitulates the transcriptional features of aging in these organs at the whole-tissue-level and the individual cell population level, including non-immune cell populations. Shared features include both inflammation signals themselves but also many genes not traditionally connected with inflammation, demonstrating a broader “aging” effect of CI. We further show that senolytic treatment, which reverses some aspects of aging by reducing senescent cell load, also reverses the gene expression changes shared between aging and CI. These results suggest that instead of merely being caused by molecular changes related to aging, CI is (also) an upstream driver of aging that causes some of the cellular and molecular changes of aging. This underscores the therapeutic potential of targeting CI to counter aging-related phenotypes.

Results

1. Chronic inflammation in the young recapitulates age-related transcriptome changes in lung, liver and kidney

To test if CI recapitulates aspects of aging, we first compared bulk gene expression profiles of aging mice organs to the gene expression profiles of the same organs from young mice exposed to CI-eliciting interventions. We use publicly available data from 4 independent studies, covering aging and CI in 3 organs: lung, liver and kidney.

The CI models used were (1) idiopathic pulmonary fibrosis, characterized by the thickening

Source	Tissue	Context	Intervention	# mice
The Tabula Muris Consortium 2020 (senis)[11]	Lung	Aging	24/27 months vs 3 months	8 vs 7
Matsuda et al. 2020[8]	Lung	Pulmonary fibrosis	Mock treated vs bleomycin-mediated lung injury, 8 days post	3 vs 3
The Tabula Muris Consortium 2020 (senis)[11]	Liver	Aging	24/27 months vs 3 months	7 vs 6
Xiong et al. 2019[9]	Liver	Non-alcoholic steatohepatitis (NASH)	Normal chow vs NASH diet 3 months vs normal chaw	3 vs 3
The Tabula Muris Consortium 2020 (senis)[11]	Kidney	Aging	24/27 months vs 3 months	8 vs 5
Arvaniti et al. 2015[10]	Kidney	Obstructive uropathy	Mock treated vs unilateral ureter obstruction (UUO) for 8 days	6 vs 4

Table 1: Data sources for bulk RNA sequencing of aging and chronic inflammation in mice.

and stiffening of lung tissue and inflammation, induced by bleomycin instillation[8]; (2) non-alcoholic steatohepatitis (NASH), a liver disease characterized by excessive fat build-up and inflammation, induced by a high-fat, low-chlorine diet [9]; (3) obstructive nephropathy, a kidney disease characterized by progressive fibrosis and inflammation, induced by unilateral ureter obstruction [10] (Table 1).

Aging data for these 3 organs was retrieved from the *Tabula muris senis* project [11]. Together, the data comprise 12 experimental groups (3 organs x 2 studies x 2 experimental conditions).

To compare gene expression profiles of aging and CI, we identified differentially expressed genes (DEGs) separately in each study using DESeq2 [12] (Supplementary Table 1). Within each organ, there was a larger-than-expected-by-chance overlap between aging-related and CI-related sets of DEGs (hypergeometric test $p < 1.0 \times 10^{-16}$) (Fig 1 a).

Next, we correlated the ranked gene expression fold-change vectors of old/young, hereinafter O/Y, and CI/control, hereinafter CI/CTL, for aging-related DEGs, using spearman correlation. All three organs show a positive correlation coefficient ($\rho = 0.29, 0.32, 0.61$ for lung, liver and kidney respectively, $p < 1.0 \times 10^{-16}$ for all three). The correlation is visualized by a density map which shows high density along the diagonal (Fig 1 b). Additionally, examining the overlapping set of O/Y and CI/CTL DEGs, we find that most are correlated (O/Y up & CI/CTL up, O/Y down & CI/CTL down) rather than anti-correlated (O/Y up & CI/CTL down, O/Y down & CI/CTL up) in all three organs (Fig 1 c). These correlations indicate that a sizable fraction of the gene expression changes that occur in aging are recaptured by CI.

Figure 1

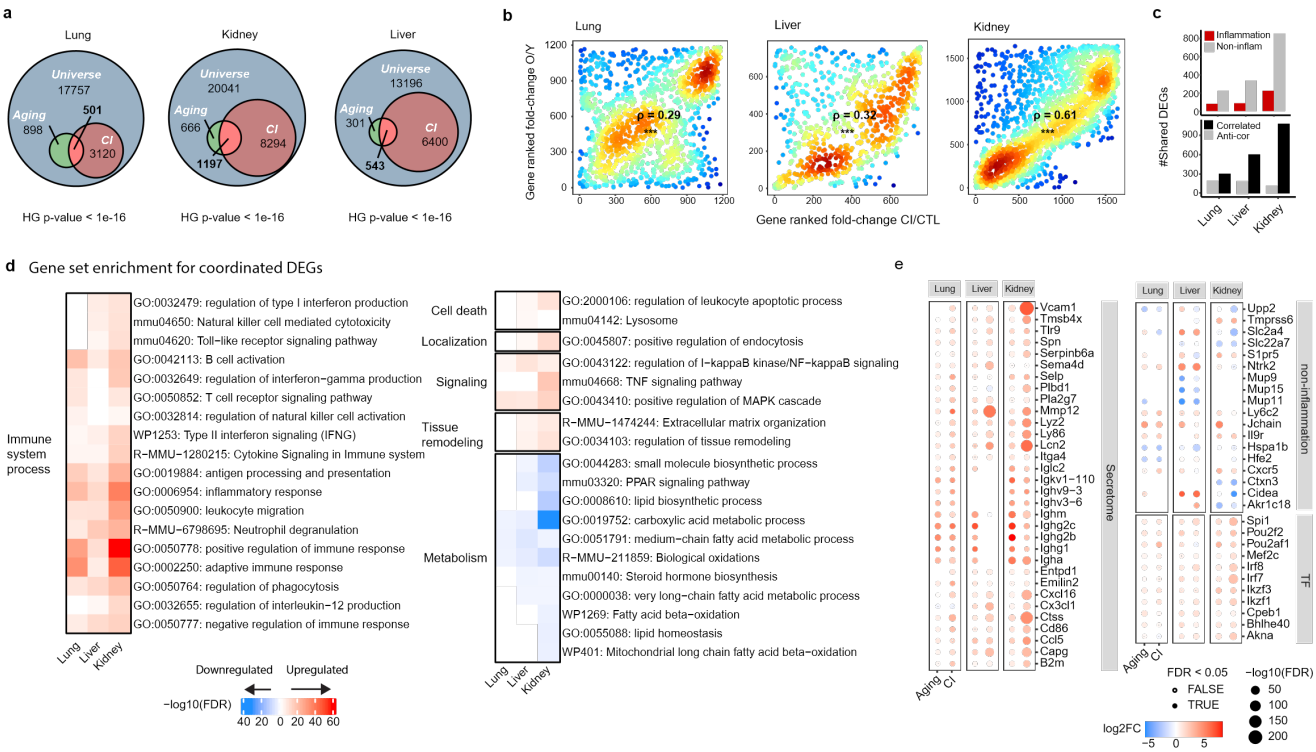

Fig. 1: Chronic inflammation recapitulates age-related bulk transcriptomic changes in lung, liver and kidney.

a, Euler diagram depicting overlap of DEG sets for O vs. Y and CI vs CTL for lung, liver and kidney. Hypergeometric test for overlap $p < 1.0 \times 10^{-16}$ for all. **b**, Ranked mean fold-changes for CI/CTL (x-axis) and O/Y (y-axis) gene expression for aging DEGs shown on a density map for lung, liver and kidney. Spearman correlation coefficient 0.29, 0.32 and 0.61 respectively. $p < 1.0 \times 10^{-16}$ for all. **c**, DEGs from the 3 overlap regions of the Euler diagrams, divided into DEGs that change in correlated (++, --) or anti-correlated (+-, -+) manners (bottom), and the correlated DEGs to inflammation- and non-inflammation-related (top). **d**, Selected enriched gene sets for correlated DEGs from the overlap regions of the Euler diagrams. Heatmap is color-coded for $-log10(FDR)$. Red designates increasing genes, blues decreasing. **e**, Transcription factors and secreted factors upregulated in aging and CI in at least two organs, and top-FC non-inflammation factors. Color code depicts fold-change in expression, circle size depicts $-log10(FDR)$ and circle fill signifies statistical significance.

In order to characterize the biological processes shared by aging and CI, we used MetaScape [14] to test for enrichment of gene sets in the shared correlated DEGs (up- and downregulated) in each organ (Fig. 1 d, Supplementary Table 2, also see methods). The shared upregulated DEGs were enriched for immune system processes and signaling pathways in all 3 organs. Immune processes included both innate and adaptive immunity, i.e., antigen presentation, Type I/II interferon signaling, neutrophil degranulation and phagocytosis, as well as T cell and B cell activation. Implicated signaling pathways include MAPK/ERK, NF-KappaB and TNF. In addition, in liver and kidney, cell death related pathways and endocytosis are upregulated, as well as extracellular matrix related pathways.

Downregulated pathways are dominated by metabolic processes, and specifically lipid and fatty acid metabolism (Fig. 1 d).

Importantly, the shared DEGs consist not only of inflammation-related genes (Fig 1 c, Methods), but also of metabolic, structural and signaling genes, implying a broader “aging” effect of CI on gene expression beyond inflammation itself.

Finally, we ask particularly which secreted/extracellular, transcription factors and non-inflammation-related genes are shared between aging and CI. We find that secreted factors and TFs changing in at least two organs in both aging and CI are all upregulated (Fig. 1 e). Secreted factors include several immunoglobulin genes, suggesting B lymphocytes are either activated or recruited to the tissue in aging and CI. Mmp12, upregulated in all three organs, may be SASP-related [15]. TFs are enriched for immune modulators, including Irf7/8, Ikzf1/3, Pou2f2 and Pou2af1.

Overall, we observed broad pan-organ and some organ-specific gene expression changes shared by aging and CI. The upregulation of immune-related pathways in aging and CI in all organs implies either infiltration of immune cells into the organ or activation of resident immune cells, which accords well with expectation. However, distinguishing activation from infiltration is a non-trivial task using bulk RNA sequencing data, which represents a mixture of multiple cell populations comprising the organ. To resolve changes at the cell population

Source	Tissue	Context	Intervention	# mice used for downstream analysis	Clustering & annotation	Cell population for downstream analysis	# O	# Y	# CI	# CTL
Angelidis et al. 2019[19]	Lung	Aging	24 months vs 3 months	8 vs 7	Published					
						Alveolar macrophage (AM)	516	1182	3271	1055
Strunz et al. 2020[16]	Lung	Pulmonary fibrosis	Bleomycin-mediated lung injury (7-56 days post) vs mock treated	40 vs 9	Published	Alveolar type II pneumocyte (AT2)	1179	2981	7517	4081
						B cell	653	192	658	213
						Capillary endothelial cell (CEC)	120	88	83	85
						Ciliated cell	489	383	5024	643
						Club cell	126	623	4694	732
						Dendritic cell (DC)	265	347	2298	307
						Fibroblast	35	54	243	90
						Goblet cell	87	186	1015	184
						Granulocyte	253	53	366	67
						Lymphatic endothelial cell (LEC)	15	41	198	49
						Macrophage	270	178	5982	204
						Mesothelial cell	127	151	471	154
						Monocyte	439	68	94	65
						Natural killer cell (NK)	67	122	70	145
						Plasma cell	156	20	222	17
						Smooth muscle cell (SMC)	30	47	85	48
						T cell	908	284	1253	332
						Vascular endothelial cell (VEC)	455	390	703	377
The Tabula Muris Consortium 2020 (senis)[20]	Liver	Aging	30/24/21/18 months vs 3 months	7 vs 3	*de novo*	Hepatocyte	605	982	469	163
Xiong et al. 2019[17]	Liver	Non-alcoholic steatohepatitis (NASH)	Amylin diet 6 weeks vs normal chow	3 vs 3	*de novo*	Hepatic sinusoidal endothelial cell (HSEC)	141	19	2474	7910
						Kupffer cell	1876	12	5921	1639
The Tabula Muris Consortium 2020 (senis)[20]	Kidney	Aging	30/21/18 months vs 3 months	9 vs 3	*de novo*	Capillary endothelial cell (CEC)	39	80	134	103
Conway et al. 2020[18]	Kidney	Obstructive uropathy	Unilateral ureter obstruction (UUO) for 7 days vs sham operated vs mock treated	3 vs 3	Published	Cortex artery cell (CAC)	251	68	85	35
						Distal convoluted tubule epithelial cell (DCTEC)	519	125	226	19
						Fenestrated cell	640	181	263	68
						Loop of Henle limb epithelial cell (LHLEC)	885	358	142	18
						Macrophage	922	139	1458	30
						Mesangial cell	86	67	12	30
						Podocyte	307	98	46	49
						Proximal convoluted tubule epithelial cell (PCTEC)	2821	681	118	91
						Proximal straight tubule epithelial cell (PSTEC)	2689	290	38	127
						T cell	341	18	270	15

Table 2: Data sources for single-cell RNA sequencing of mouse aging and chronic inflammation.

level, scRNA-seq techniques are more suitable. We next turn to analysis of scRNA-seq datasets for aging and CI.

2. CI recapitulates age-related gene expression changes at the level of individual cell populations analyzed by scRNA-seq

To examine cell population-specific changes shared by aging and CI in lung, liver and kidney, we analyzed scRNA-seq data for aging and for CI-inducing interventions (similar to the bulk analysis). CI data in young mice was retrieved from 3 independent studies: (1) a study by *Strunz et al.* [16] charting the cellular dynamics of bleomycin-mediated lung injury, which induces fibrosis and CI, comprising 63,872 cells from 64 mice; (2) a study by *Xiong et al.* [17], which sequenced 33,168 cells from the livers of 3 mice that were on 6 weeks amylin diet, which recapitulated key features of human NASH, and 3 controls; (3) atlas of kidney disease by *Conway et al*. [18], comprising 8,410 cells from 3 mice that underwent unilateral ureter obstruction for 7 days, and 3 sham-treated controls.

Aging data was retrieved from (4) atlas of murine lung aging by *Angelidis et al.* [19], comprising 14,813 cells collected from 15 mice; (5) The *tabula muris senis* project [20], which sequenced 5,924 cells from mouse liver and 10,280 cells from mouse kidney in different ages. All data sources are described in Table 2. The cells from each organ are depicted in a 2-dimensional t-distributed stochastic neighbor embedding (t-SNE) plot color coded for cell population or experimental group (Supplementary Fig. 1 a-c, methods).

Broad cell population annotations are adopted from original publications and merged, or re-established here using the Seurat V4 [21] package suite (see methods). We retained a coarse-grained annotation in order to simplify the cross-dataset-matching process (Supplementary fig 1 d-f).

A total of 28, 19, and 26 cell populations were identified in lung, liver and kidney, respectively (Supplementary Fig. 1 a-c, Supplementary Table 3-8). Due to biological factors and to different tissue-processing protocols implemented in the studies, studies differ in the fraction of cells from each population. A population that is abundant in one dataset may be absent from another. We therefore focused on cell populations where at least 10 cells are present from each of the four experimental groups, namely O, Y, CI and CTL. In lung, a total of 19 cell populations met this criterion (Table 2), covering parenchymal tissue (alveolar type 2 pneumocytes (AT2)), epithelial tissue (ciliated cells, club cells, goblet cell), lymphocytes (T cells, natural killer cells (NK) B cells, plasma cells), myeloid cells (circulating macrophages, alveolar macrophages (AM), dendritic cells (DC), granulocytes, stromal cells (capillary, vascular and lymphatic endothelial cells (C/V/LEC), fibroblasts, mesothelial cells) and smooth muscle cells (SMC). In the liver, 3 populations met this criterion (Table 2): Kupffer cells, hepatocytes, and hepatic sinusoid endothelial cells (HSEC). In Kidney, 11 cell populations met the criterion (Table 2): capillary endothelial cell (CEC), cortex artery cells (CAC), distal convoluted tubule epithelial cell (DCTEC), fenestrated cells, loop of Henle limb epithelial cell (LHLEC), mesangial cell, proximal convoluted tubule epithelial cell

(PCTEC), proximal straight tubule epithelial cell (PSTEC), podocytes, T cell, and macrophages (Table 2).

First, we removed ambient mRNA (see Methods) to avoid spurious DEGs. Next, we performed differential gene expression analysis on old vs. young and CI vs. healthy, using MAST [22] on log-normalized expression values controlled for sex ($|log2\ fold-change| > 0.32,\ FDR < 0.05$, methods).

Consistent with bulk analysis, we observe positive spearman correlations in the range of 0.2-0.8 between the ranked gene expression fold-change vectors (O/Y, CI/CTL) of aging-related DEGs. This applies to multiple cell populations (Fig. 2 a, Supplementary Fig. 1 g) in all three organs. There are more correlated than anti-correlated shared DEGs in almost all cell populations (Fig. 2 a, Supplementary Table 9). These results indicate CI in the young recapitulates of aging gene expression changes also at the cell population level. DEGs include both inflammation and non-inflammation-related genes, demonstrating that the recapitulation extends beyond inflammation signals themselves (Fig. 2 a, Supplementary Table 9).

The most robust DEGs, shared by 4 or more cell populations, are presented in a heatmap (Fig. 2 b). There are more upregulated than downregulated shared DEGs, and few inconsistent DEGs (e.g., up in one cell population and down in another). The map is dominated by immune-related genes, which is the shares signal most robust across populations. Notably, alterations in antigen presentation are a common feature of aging and CI. B2m and H2-K1, encoding for the MHC class I protein complex, are upregulated in both immune (e.g., alveolar macrophage) or non-immune (e.g., AT2) cells. Genes encoding for the MHC class II protein complex (H2- Eb1/Ae/DMb1/Ab1, Cd74) are upregulated in alveolar macrophages, kupffer cells, kidney T cells and also in fenestrated cells. Endothelial cells are known to express MHC class II in some contexts [23]. Interestingly, lung dendritic cells and renal macrophages seem to downregulate this antigen-presentation pathway.

Three members of the pro-inflammatory circulating S100 family (a6/8/9) are upregulated in a number of cell populations. S100a9 is known to be elevated in mammalian aging [24]. Several polymorphisms of ApoE, upregulated in Kupffer cells, DCTECs, CACs, PSTECs, and HLHECs, have been associated with Alzheimer's[25] and with longevity [25, 26].

Several genes are notably downregulated in multiple populations, including Inmt, Glul, Rnase4, Sult1a1, Gm9846 and Gm10263. Tmsb10 is upregulated in kidney endothelial cells and downregulated in immune cells.

Consistent with results obtained from bulk data, pathway analysis applied to specific populations (Fig. 2 c, Supplementary Table 10) reveals upregulation of immune system processes, e.g., antigen presentation (class I and class II), phagosome, cytokine production, interferon-gamma/TNF/MAPK/ERK signaling, and neutrophil degranulation, as well as cell death. Uniquely to single cell analysis, we observe an upregulation of antigen presentation (class I and class II) in non-immune cells, as well as angiogenesis signals, cell adhesion,

growth arrest and cellular senescence, and oxidative stress and redox, which accords with redox imbalances often associated with aging [28] and with CI [29].

Figure 2

Fig. 2: Chronic inflammation recapitulates age-related gene expression changes at the level of individual cell populations analyzed by scRNA-seq.

a, From left to right: total number of DGEs in aging and CI studies combined; DGE fraction shared vs study specific; Spearman correlation of O/Y and CI/CTL ranked mean gene expression fold-changes for aging DEGs, where > 10 are present (otherwise denoted na); DEG correlation (black: ++, --, grey: +-, -+); inflammation and non-inflammation related fractions of correlated DEGs. Separated by organ and color coded. **b**, Aging/CI DEGs that are shared for 3 or more cell populations. Color coded for pattern. na = none of the above. **c**, Gene sets most consistently enriched in DEG lists across cell populations. Red designates increasing genes, blues decreasing.

Also consistent with bulk data, lipid metabolism/catabolism is downregulated in four populations (Fig. 2 c).

Overall, CI in young animals recapitulates multiple transcriptional changes observed in aging in different cell populations, including immune, parenchymal and stromal populations, in a pan-organ manner. Shared DEGs and gene sets include both inflammation signals themselves and non-inflammation-related factors.

3. Senolytic treatment partially reverses age-related transcriptional changes that are shared with CI in lung, liver and kidney, and decreases transcriptional age

To further test the hypothesis that CI recapitulates aspects of aging, we studied the effects of an intervention that reverses some aspects of aging in mice: a drug that remove senescent cells, known as a senolytic drug [30]. We used data from *Ovadya et al.* [13] where the senolytic agent ABT-737 [31] was administered to old (20 month) C57BL/6 *Perf1-/-* mice, followed by whole-tissue bulk RNA sequencing of lung, liver and kidney from the treated group, as well as old (20 months) and young (3 months) C57BL/6 *Perf1-/-* controls.

ABT-737 treatment, which eliminates senescent cells by inhibiting the anti-apoptotic BCL-2 family of proteins, attenuated transcriptional aging and prolonged lifespan of these mice [13]. Consistent with this, ABT samples fall between Y and O in a PCA plot based on normalized gene expression (Fig 3 a).

We sought to quantify how senolytic treatment affected the transcriptional changes shared by aging and CI. To do so, we computed for each organ the “rejuvenation vector”, given by the gene expression fold-changes between ABT-treated and untreated old mice, ABT/O. For aging related DEGs (Supplementary table 11), we correlated the rejuvenation vector with the “CI vector” of the effects of CI in young mice analyzed in section 1, given by fold changes CI/CTL. In all three organs the spearman correlation coefficient is negative (Fig. 3 b, $\rho < -0.4$, $p < 1.0 \times 10^{-16}$). This shows that ABT-737 senolytic treatment partially rejuvenates the CI-shared component of aging.

Next, we examined the intersection of the DEG sets (Supplementary table 11) for aging, CI and ABT-737 treatment in each organ. Of 8 possible trends in this gene set (each gene can be up or down regulated in ageing, CI and ABT-373), we find that nearly all genes are either upregulated in aging and CI and downregulated in ABT-737 treatment, or vice versa (Fig. 3 c). We conclude that this DEG set is mainly composed of genes "rejuvenated" by ABT-737 treatment, with the majority being downregulated.

We tested which of the enriched gene sets detected in our original analysis are rejuvenated by ABT-737 (Supplementary table 12). We find that multiple immune-related changes are diminished by the senolytic, as are cell death, TNF and MAPK signaling (Fig. 3 d). Some of the metabolic and biological oxidation pathways are increased. This is again consistent with the hypothesis that senolytic rejuvenates processes shared by CI and aging. Several secreted factors and TFs are rejuvenated, notably Tmsb4x, Ctss, Ccl5, and Irf7 are rejuvenated in both

liver and kidney. Leading non-inflammation-related aging/CI DEGs are slightly affected (Fig. 3 d).

Figure 3

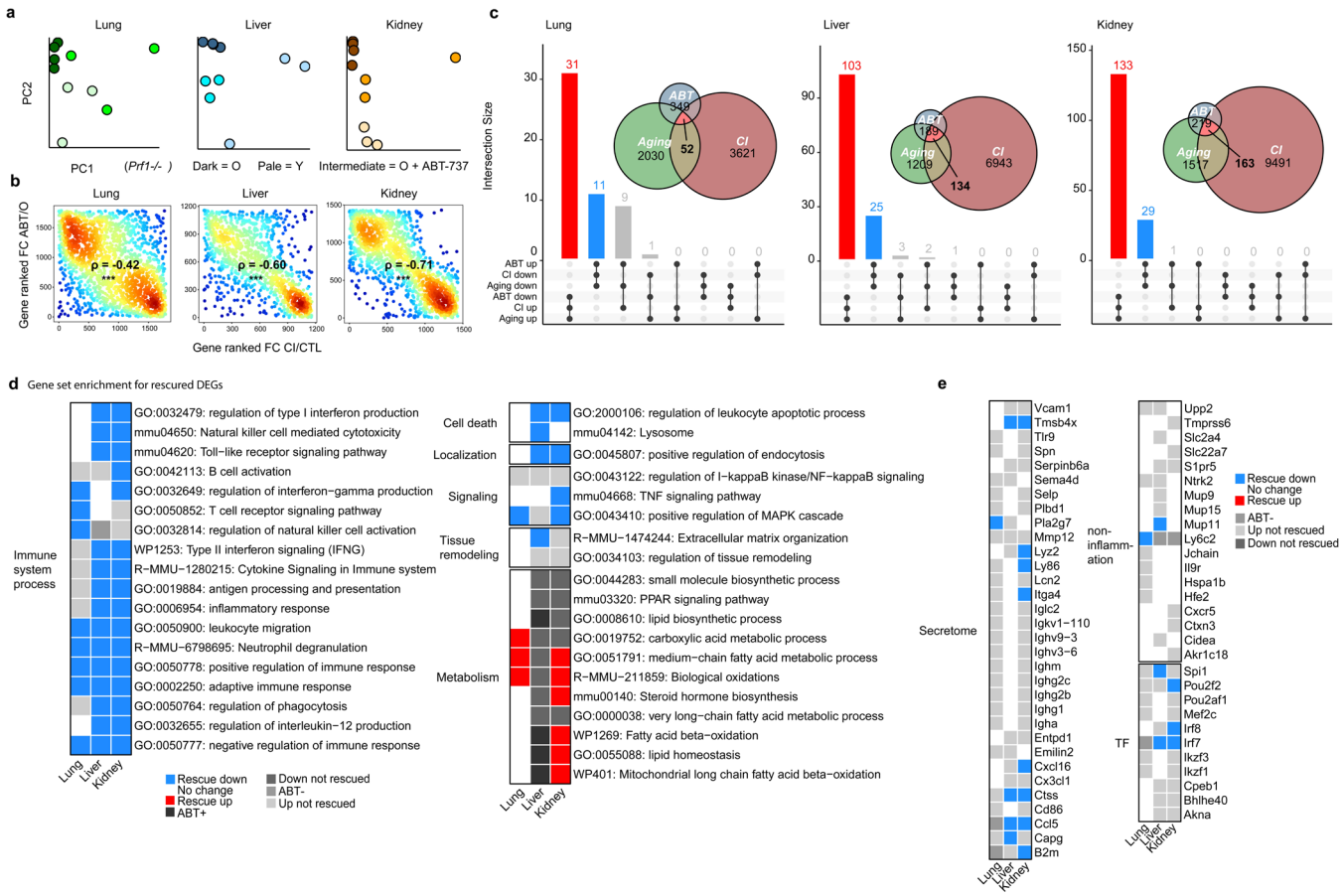

Fig. 3: Senolytic treatment rejuvenates age-related transcriptional changes that are shared with Chronic inflammation in lung, liver and kidney.

a, PCA of samples based on normalized gene expression of young, old, and ABT-737-treated old Perf1-/- mice separately from three organs. **b**, Ranked mean fold-changes CI/CTL (x-axis) and ABT/O (y-axis) gene expression for aging DEGs shown on a density map for lung, liver and kidney. Spearman correlation coefficient -0.42, -0.60 and -0.71 respectively. $p < 1.0 \times 10^{-16}$ for all. **c**, Euler diagram depicting overlap of DEG sets for O vs. Y and CI vs. CTL and ABT vs. O for lung, liver and kidney. Upset plot showing interaction of the gene sets. **d**, Enriched gene sets for rescued DEGs from c, color coded accordingly. **e**, Transcription factors, secreted factors, and non-inflammation-related factors rescued by ABT-737 in three organs, color coded as in d.

Finally, we evaluated the RNA age of these samples by means of RNAAgeCalc [32], a transcriptional age calculator. RNAAgeCalc was calibrated for different human organs, so for the purpose of our analysis we converted mouse gene names to their human homologs and scaled the age readout. Interestingly, we observe that for all three tissues, the clock assigns higher RNA age to O compared to Y mice, and to CI compared to CTL, while ABT-treated animals fall between Y and O (Fig 4 a). These results match our expectation, notwithstanding

pan-species application. This underscores the notion that the shared component of aging and CI is a strong determinant of transcriptional age in mammals.

Figure 4

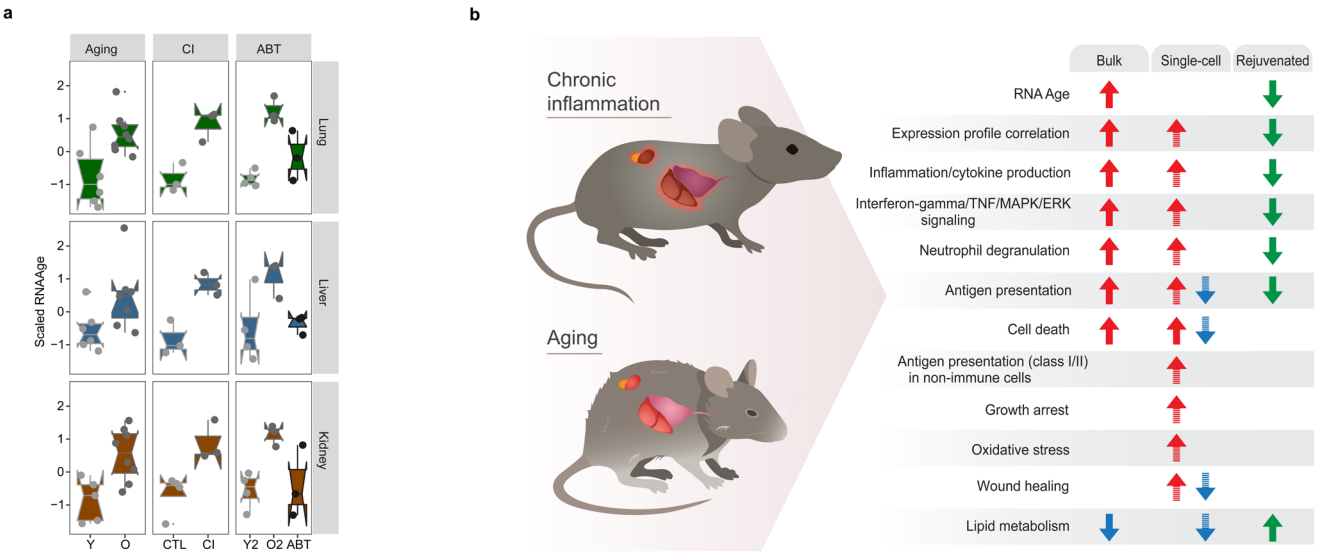

Fig. 4: Chronic inflammation increases RNA age, and illustrated summary of results.

a, RNAAgeCalc aging clock applied to data analyzed in this study and scaled. **b**, Illustration of the main results of the study.

Discussion

We tested the hypothesis that mammalian aging is recapitulated by CI in young organisms. To do so, we compared gene expression signature of aging mice to that of CI in young mice using bulk and single-cell gene expression datasets. We find that aging signature is correlated with CI signature. CI partially recapitulates age-related gene expression changes in both in immune and non-immune cells, and with respect to inflammation and non-inflammation-related genes. Specific shared transcriptional programs include inflammation/cytokine production, interferon-gamma/TNF/MAPK/ERK signaling, neutrophil degranulation, cell death, antigen presentation (class I/II) in non-immune cells, growth arrest, oxidative stress and wound healing. Lipid metabolism is the only pathway that is consistently downregulated (Fig. 4 b). Together, these findings suggest that CI may cause aging phenotypes and not just be caused by molecular and cellular damage associated with ageing.

Downregulation of lipid and fatty acid metabolism and associated PPAR signaling is a strong shared aspect of aging and CI in our analysis. Indeed, an emerging body of data suggests that lipid metabolism plays a role in the aging process. In humans, adiposity increases with age [33]. In a range of model organisms, dietary, pharmacological, genetic, and surgical lipid-related interventions extend lifespan [34]. Studies in mice also demonstrated the other side of the coin,

that high-fat diet accelerates aging [35]. It is thus notable that our analysis indicates that lipid metabolism decrease is also a salient feature of CI.

Another notable process shared by aging and CI is an increase in class I and class II antigen-presentation, which occurs in both immune subtypes and in endothelial and epithelial cells.

While canonical cellular senescence markers Cdkn1a and Cdkn2a did not emerge as shared features of aging and CI, we find that other senescence associated genes, e.g., inflammatory cytokines and matrix metalloproteinases, are upregulated (Fig 1 e), and so are pathways relating to cell-cycle arrest and cellular senescence in the single-cell analysis (Fig 2 c). 24 of 119 murine *in vivo* senescence-related genes curated in SenMayo gene set [36] are upregulated in kidney aging and CI in bulk analysis (supplementary Table 1), of which Jun and Spp1 are also upregulated specifically in fenestrated cells and in proximal straight/convoluted tubule epithelial cell (Fig 2 b). In addition, MAPK, upregulated in both whole-organ and in several specific cell-populations, and NF-κB signaling pathways, upregulated whole-organ levels, have been implicated as pro-senescence and as potential SASP regulators [37–40]. TNF signaling, which is upregulated in the kidney on whole organ and cell population levels, is also associated with SASP [41].

Consistent with our findings, a recent analysis of transcription factors regulatory activity based on TMS dataset [42] also reported upregulation of Nfkb1, TNF-signaling genes, and antigen processing machinery to be robust features of aging. Increased regulatory activity of Nfkb1 was experimentally verified in kidney using ChIP–seq.

It is worth noting that age-related changes in gene expression likely consist of both (1) passive non-coordinated drift of the gene expression, and (2) a concomitant coordinated stress response meant to counter various damage types incurred to the organism and to restore homeostasis. Pathway analysis highlights the coordinated, responsive, changes.

To further test the link between aging and CI, we analyzed an experiment in which a senolytic drug was used to remove senescent cells from aged mice. This treatment reversed much of the gene expression changes shared between aging and CI. Thus, removal of senescent cells can be interpreted as removing a major source of inflammaging. This accords well with a study showing systemic senolysis, by either genetic or pharmaceutic means, reduced brain microglial activation and SASP and alleviates cognitive impairment in mice [43].

Finally, we observed an acceleration of transcriptional age in all three organs induced with CI, and that transcriptional age is decreased in aging by inflammation-reducing senolytic treatment. In humans, accelerated epigenetic aging (measured by DNA methylation clock [44]) has been associated with tobacco use [45], HIV [46] and Covid-19 infection [47]. Since these three conditions involve CI, and in light of our findings, it is reasonable to suggest that the reported DNA methylation age acceleration is at least in part inflammation-mediated. Along the same lines, it was recently shown that even transient inflammatory stimulus accelerates aging of hematopoietic stem cells, manifesting in increased epigenetic age and long-lasting impaired self-renewal [48]. Another recent study has, however, shown that inflammation (measured using

blood borne factors) and epigenetic aging are largely independent markers of aging [49]. More work is required to elucidate the relationship between these important aging markers.

Although CI is well studied in the context of aging [1], and although it was shown previously that inflammation is a robust gene-expression hallmark of aging in different organs [50] and mammalian species [51], by directly comparing aging and CI in young, our approach offers new insights into the wide-ranging effect of CI. We show that CI affects the gene expression signature of immune and non-immune cells to look more like aged cells, with respect to inflammation-related and unrelated genes. Another study showed a similar overlap between aging and oncogenic gene signatures in human cancers [52]. A potentially revealing future analysis can examine the nexus of aging, CI and cancer.

A major technical challenge we faced was comparing datasets generated in different studies. Technical inter-study differences, e.g., protocols and batch effects, may mask biological correspondence. We note that the correlations found here, many exceeding 0.5, are at least as large as in a 'positive control' analysis comparing the same biological process - aging - from two different studies, in both bulk and single-cell levels (see Supplementary material, Figs. 2-3). We thus both recognize this as a limitation of our methodology, and as a reminder that the actual correspondence between aging and CI may be even stronger than described.

Another limitation of this study is that the senolytic treatment is only analyzed in bulk level (owing to lack of single-cell studies), which does not allow us to determine if the observed reversal of gene expression changes derives from compositional changes of the tissue, or changes in specific cell populations, or a combination (most likely option).

The present findings relate to a fundamental question: Are there ultimate drivers of aging? An ultimate driver is a factor that increases over the lifespan, and which drives multiple proximal aspects of aging. The finding that CI partially recapitulates gene expression changes in aging may point towards one potential ultimate driver. This driver is the accumulation of cells in the body that secrete inflammatory signals. Such cells include senescent cells which secrete SASP, a cocktail of potent inflammatory signals. Other types of damaged cells may also participate and secrete inflammatory factors.

Along these lines, it was recently shown that inflammation can decouple cancer risk and other aging phenotypes from chronological age. In young women carrying BRCA1/2 germline mutations, known to cause susceptibility to breast cancer, breast tissue presents cell lineage fidelity loss concomitant with inflammatory markers, similar to breast tissue of older women [53]. In this context, inflammation may perturb homeostatic cues, driving cells to explore cellular states conducive to clonal expansion, altered identities and progression of carcinogenesis [54].

One may ask why do inflammation markers rise over the lifespan in the first place? What is the fundamental reason for the rise of the number of pro-inflammatory cells such as senescent cells? One plausible mechanism is the linear increase with age of alterations in stem cells, including epigenetic changes, mutations and retroviral events [55]. In young humans and mice,

stem cells bear virtually no epigenetic changes or mutations, whereas as at old age (80y old humans, 2y old mice) each stem cell harbors several thousand mutations on average[5657] and widespread epigenetic changes [56]. Over time, more and more stem cells become altered in a way that disrupts genes expressed in their differentiated progeny. These alterations cause damage in the differentiated cells, driving the differentiated cells to become senescent and to secrete inflammatory signals.

Senescent cell production thus rises with age, eventually saturating the senescent cell removal mechanisms [6]. Once removal of senescent cells is saturated, senescent cell levels and their inflammatory secretions increase strongly with age. Mathematical modeling of this process indeed captures many quantitative hallmarks of aging and age-related diseases [58].

To conclude, our findings support a hypothesis that inflammaging lies downstream of cellular changes associated with ageing, instead of being caused by them. Proposed drivers and hallmarks of aging that are commonly considered to cause inflammaging, may in fact also be caused by it. This explains why reduction of inflammaging by removal of senescent cells has wide-ranging beneficial effects on multiple dysfunctions of aging. The present findings also call for better understanding of the pathways by which chronic inflammation carries out its broad effects on organelles, cells and organs. Such pathways may serve as targets for interventions to mitigate age-related decline.

Methods

Bulk differential gene expression analysis: for differential gene expression analysis, we used DESeq2 standard workflow, which is based on the negative binomial distribution. Set interactions in figure 3 were visualized with R UpSetR code package [60].

Bulk gene set analysis: shared DEG lists were analyzed with MetaScape web interface [14] for multiple gene lists with Min Overlap = 2, P Value Cutoff = 0.01, and Min Enrichment = 1.5.

Sc clustering and cell-population annotation: cell-population annotations were adopted from original studies when applicable (lung:Strunz/Angelidis, kidney:TMS). Where published annotation was deemed too coarse-grained (lung:TMS, liver:Xiong/TMS, kidney:Conway), Seurat package (version 4.0) [61] standard workflow was used to cluster. Briefly, UMI matrix was log-normalize, highly variable genes were detected, and PCA was applied, followed by KNN graph construction on 50 leading components. Louvain algorithm was used for community detection using resolution parameter 1.5. Clusters were manually annotated based on marker genes and cross-reference with the pre-annotated dataset. Note that not all mice used for clustering are used for downstream analysis.

All TMS data used for this and subsequent analysis was generated using microfluidic droplet technology (10X Genomics).

Sc ambient RNA removal: ambient RNA is RNA present in the cell suspension that can be aberrantly counted along with a cell's native mRNA. In most datasets, ubiquitous expression

of highly-expressed cell-type specific genes (e.g surfactant genes in lung tissue), suggested such cross-contamination. To overcome this, decontX() function from celda (V1.6.1) [62] was used with default parameters to remove contamination in individual cells. decontX is a Bayesian method that models the empirical expression of a cell is a mixture of counts from two multinomial distributions: (1) a distribution of native transcript counts from the cell's actual population and (2) a distribution of contaminating transcript counts from all other cell populations captured in the assay.

Sc 2-dimentional representation: For generating the tSNE maps of single-cells, the Seurat V4 [61] RunTSNE() function was used with these parameters: dims = 1:50, reduction = "pca".

Sc differential gene expression analysis: Two-sided MAST test implemented in Seurat V4 was applied to decontaminated log-transformed normalized counts for each group and each cell-population individually. Genes were tested if they are expressed in > 0.01 of cells and with > 5 cells with > 1 UMIs. DGEs are selected to be $|fold - change| > 1.25$, Benjamini-Hochberg adjusted $P < 0.05$. Tests were controlled for sex as a covariant.

In order to avoid ambient RNA, in addition to using DecontX corrected data, we also discounted genes if they met both these criteria: 1. among the top 5 markers in another cell-population *and* 2. among the top 50 most highly expressed genes in the dataset.

We note that for Strunz et al. lung fibrosis study, who performed timecourse measurements, we used cells from 7 days post- bleomycin treatment onwards.

For liver and kidney, tests were applied for old vs. young where "old" consists of cells pooled from 18-, 21-, 24- and 30-month-old mice, and "young" consisted of 3-month-old mice.

Inflammation-related gene set: chosen as "inflammatory response" gene ontology term (GO:0006954), combined with genes prefixed: Irf, Ifi, H2-, C1q, Cd(digit), Igj, Igh, Igk, Igl.

Sc gene set enrichment analysis: shared DEG lists were analyzed with MetaScape web interface for multiple gene lists with Min Overlap = 2, P Value Cutoff = 0.01, and Min Enrichment = 1.5.

RNA age calculation: RNA age was calculated using RNAAgeCalc [32] trained on human data derived from GTEx V6 to construct our across-tissue and tissue-specific transcriptional age calculator. The algorithm was implemented in R following the guidelines described in https://www.bioconductor.org/packages/release/bioc/vignettes/RNAAgeCalc/inst/doc/RNAAge-vignette.html, with lung specific predictor used for lung and pan-tissue predictor used for liver and kidney, while supplying the counts matrix. Mouse genes are converted to human homologs by simple case-matching. The readout, given in human years, was scaled for presentation.

Code availability

Custom code will be supplied upon reasonable request.

Competing interests statement

The authors declare no competing interests.

References

1. Franceschi, C. & Campisi, J. Chronic Inflammation (Inflammaging) and Its Potential Contribution to Age-Associated Diseases. *J. Gerontol. Ser. A* **69**, S4–S9 (2014).
2. Furman, D. *et al.* Chronic inflammation in the etiology of disease across the life span. *Nat. Med.* **25**, 1822–1832 (2019).
3. Ferrucci, L. & Fabbri, E. Inflammageing: chronic inflammation in ageing, cardiovascular disease, and frailty. *Nat. Rev. Cardiol.* **15**, 505–522 (2018).
4. Sanada, F. *et al.* Source of Chronic Inflammation in Aging. *Front. Cardiovasc. Med.* **5**, (2018).
5. Hernandez-Segura, A., Nehme, J. & Demaria, M. Hallmarks of Cellular Senescence. *Trends Cell Biol.* **28**, 436–453 (2018).
6. Karin, O., Agrawal, A., Porat, Z., Krizhanovsky, V. & Alon, U. Senescent cell turnover slows with age providing an explanation for the Gompertz law. *Nat. Commun.* **10**, 5495 (2019).
7. López-Otín, C., Blasco, M. A., Partridge, L., Serrano, M. & Kroemer, G. The Hallmarks of Aging. *Cell* **153**, 1194–1217 (2013).
8. Matsuda, S. *et al.* Transcriptomic Evaluation of Pulmonary Fibrosis-Related Genes: Utilization of Transgenic Mice with Modifying p38 Signal in the Lungs. *Int. J. Mol. Sci.* **21**, E6746 (2020).
9. Xiong, X. *et al.* Mapping the molecular signatures of diet-induced NASH and its regulation by the hepatokine Tsukushi. *Mol. Metab.* **20**, 128–137 (2019).
10. Arvaniti, E. *et al.* Whole-transcriptome analysis of UUO mouse model of renal fibrosis reveals new molecular players in kidney diseases. *Sci. Rep.* **6**, 26235 (2016).
11. Schaum, N. *et al.* Ageing hallmarks exhibit organ-specific temporal signatures. *Nature* **583**, 596–602 (2020).
12. Love, M. I., Huber, W. & Anders, S. Moderated estimation of fold change and dispersion for RNA-seq data with DESeq2. *Genome Biol.* **15**, 550 (2014).

13. Ovadya, Y. *et al.* Impaired immune surveillance accelerates accumulation of senescent cells and aging. *Nat. Commun.* **9**, 5435 (2018).
14. Zhou, Y. *et al.* Metascape provides a biologist-oriented resource for the analysis of systems-level datasets. *Nat. Commun.* **10**, 1523 (2019).
15. Hudgins, A. D. *et al.* Age- and Tissue-Specific Expression of Senescence Biomarkers in Mice. *Front. Genet.* **9**, (2018).
16. Strunz, M. *et al.* Alveolar regeneration through a Krt8+ transitional stem cell state that persists in human lung fibrosis. *Nat. Commun.* **11**, 3559 (2020).
17. Xiong, X. *et al.* Landscape of Intercellular Crosstalk in Healthy and NASH Liver Revealed by Single-Cell Secretome Gene Analysis. *Mol. Cell* **75**, 644-660.e5 (2019).
18. Conway, B. R. *et al.* Kidney Single-Cell Atlas Reveals Myeloid Heterogeneity in Progression and Regression of Kidney Disease. *J. Am. Soc. Nephrol. JASN* **31**, 2833–2854 (2020).
19. Angelidis, I. *et al.* An atlas of the aging lung mapped by single cell transcriptomics and deep tissue proteomics. *Nat. Commun.* **10**, 963 (2019).
20. Almanzar, N. *et al.* A single-cell transcriptomic atlas characterizes ageing tissues in the mouse. *Nature* **583**, 590–595 (2020).
21. Stuart, T. *et al.* Comprehensive Integration of Single-Cell Data. *Cell* **177**, 1888-1902.e21 (2019).
22. Finak, G. *et al.* MAST: a flexible statistical framework for assessing transcriptional changes and characterizing heterogeneity in single-cell RNA sequencing data. *Genome Biol.* **16**, 278 (2015).
23. McDouall, R. M., Yacoub, M. & Rose, M. L. Isolation, culture, and characterisation of MHC class II-positive microvascular endothelial cells from the human heart. *Microvasc. Res.* **51**, 137–152 (1996).
24. Swindell, W. R. *et al.* Robust shifts in S100a9 expression with aging: a novel mechanism for chronic inflammation. *Sci. Rep.* **3**, 1215 (2013).
25. Yassine, H. N. & Finch, C. E. APOE Alleles and Diet in Brain Aging and Alzheimer's Disease. *Front. Aging Neurosci.* **12**, 150 (2020).
26. Shinohara, M. *et al.* APOE2 is associated with longevity independent of Alzheimer's disease. *eLife* **9**, e62199 (2020).

27. Reinvang, I., Espeseth, T. & Westlye, L. T. APOE-related biomarker profiles in non-pathological aging and early phases of Alzheimer's disease. *Neurosci. Biobehav. Rev.* **37**, 1322–1335 (2013).
28. Sohal, R. S. & Orr, W. C. The redox stress hypothesis of aging. *Free Radic. Biol. Med.* **52**, 539–555 (2012).
29. Chiurchiù, V. & Maccarrone, M. Chronic Inflammatory Disorders and Their Redox Control: From Molecular Mechanisms to Therapeutic Opportunities. *Antioxid. Redox Signal.* **15**, 2605–2641 (2011).
30. Wissler Gerdes, E. O., Zhu, Y., Tchkonia, T. & Kirkland, J. L. Discovery, development, and future application of senolytics: theories and predictions. *FEBS J.* **287**, 2418–2427 (2020).
31. Directed elimination of senescent cells by inhibition of BCL-W and BCL-XL | Nature Communications. https://www.nature.com/articles/ncomms11190.
32. Ren, X. & Kuan, P. F. RNAAgeCalc: A multi-tissue transcriptional age calculator. *PLOS ONE* **15**, e0237006 (2020).
33. Poehlman, E. T. *et al.* Physiological Predictors of Increasing Total and Central Adiposity in Aging Men and Women. *Arch. Intern. Med.* **155**, 2443–2448 (1995).
34. Johnson, A. A. & Stolzing, A. The role of lipid metabolism in aging, lifespan regulation, and age-related disease. *Aging Cell* **18**, e13048 (2019).
35. Honma, T. *et al.* High-fat diet intake accelerates aging, increases expression of Hsd11b1, and promotes lipid accumulation in liver of SAMP10 mouse. *Biogerontology* **13**, 93–103 (2012).
36. Saul, D. *et al.* A new gene set identifies senescent cells and predicts senescence-associated pathways across tissues. *Nat. Commun.* **13**, 1–15 (2022).
37. Cano, M., Guerrero-Castilla, A., Nabavi, S. M., Ayala, A. & Argüelles, S. Targeting pro-senescence mitogen activated protein kinase (Mapk) enzymes with bioactive natural compounds. *Food Chem. Toxicol. Int. J. Publ. Br. Ind. Biol. Res. Assoc.* **131**, 110544 (2019).
38. Freund, A., Patil, C. K. & Campisi, J. p38MAPK is a novel DNA damage response-independent regulator of the senescence-associated secretory phenotype. *EMBO J.* **30**, 1536–1548 (2011).
39. Haga, M. & Okada, M. Systems approaches to investigate the role of NF-κB signaling in aging. *Biochem. J.* **479**, 161–183 (2022).

40. Zhang, L. *et al.* Novel small molecule inhibition of IKK/NF-κB activation reduces markers of senescence and improves healthspan in mouse models of aging. *Aging Cell* **20**, e13486 (2021).
41. Parish, S. T., Wu, J. E. & Effros, R. B. Modulation of T Lymphocyte Replicative Senescence via TNF-α Inhibition: Role of Caspase-3. *J. Immunol.* **182**, 4237–4243 (2009).
42. Maity, A. K., Hu, X., Zhu, T. & Teschendorff, A. E. Inference of age-associated transcription factor regulatory activity changes in single cells. *Nat. Aging* **2**, 548–561 (2022).
43. Ogrodnik, M. *et al.* Whole-body senescent cell clearance alleviates age-related brain inflammation and cognitive impairment in mice. *Aging Cell* **20**, e13296 (2021).
44. Horvath, S. & Raj, K. DNA methylation-based biomarkers and the epigenetic clock theory of ageing. *Nat. Rev. Genet.* **19**, 371–384 (2018).
45. Beach, S. R. H. *et al.* Methylomic Aging as a Window onto the Influence of Lifestyle: Tobacco and Alcohol Use Alter the Rate of Biological Aging. *J. Am. Geriatr. Soc.* **63**, 2519–2525 (2015).
46. Boulias, K., Lieberman, J. & Greer, E. L. An Epigenetic Clock Measures Accelerated Aging in Treated HIV Infection. *Mol. Cell* **62**, 153–155 (2016).
47. Cao, X. *et al.* Accelerated biological aging in COVID-19 patients. *Nat. Commun.* **13**, 2135 (2022).
48. Bogeska, R. *et al.* Inflammatory exposure drives long-lived impairment of hematopoietic stem cell self-renewal activity and accelerated aging. *Cell Stem Cell* (2022) doi:10.1016/j.stem.2022.06.012.
49. Cribb, L. *et al.* Inflammation and epigenetic ageing are largely independent markers of biological ageing and mortality. *J. Gerontol. Ser. A* (2022).
50. de Magalhães, J. P., Curado, J. & Church, G. M. Meta-analysis of age-related gene expression profiles identifies common signatures of aging. *Bioinformatics* **25**, 875–881 (2009).
51. Palmer, D., Fabris, F., Doherty, A., Freitas, A. A. & de Magalhães, J. P. Ageing transcriptome meta-analysis reveals similarities and differences between key mammalian tissues. *Aging* **13**, 3313–3341 (2021).

52. Saul, D. & Kosinsky, R. L. Single-Cell Transcriptomics Reveals the Expression of Aging-and Senescence-Associated Genes in Distinct Cancer Cell Populations. Cells. 2021; 10: 3126. *Aging Cell* **18**, e13041 (2019).
53. Shalabi, S. F. *et al.* Evidence for accelerated aging in mammary epithelia of women carrying germline BRCA1 or BRCA2 mutations. *Nat. Aging* **1**, 838–849 (2021).
54. Caruso, J. A. & Tlsty, T. D. Remaining true to one's identity. *Nat. Aging* **1**, 757–759 (2021).
55. Enge, M. *et al.* Single-Cell Analysis of Human Pancreas Reveals Transcriptional Signatures of Aging and Somatic Mutation Patterns. *Cell* **171**, 321-330.e14 (2017).
56. Milholland, B., Suh, Y. & Vijg, J. Mutation and catastrophe in the aging genome. *Exp. Gerontol.* **94**, 34–40 (2017).
57. Cagan, A. *et al.* Somatic mutation rates scale with lifespan across mammals. *Nature* **604**, 517–524 (2022).
58. Katzir, I. *et al.* Senescent cells and the incidence of age-related diseases. *Aging Cell* **20**, e13314 (2021).
59. Stacklies, W., Redestig, H., Scholz, M., Walther, D. & Selbig, J. pcaMethods a bioconductor package providing PCA methods for incomplete data. *Bioinformatics* **23**, 1164–1167 (2007).
60. Conway, J. R., Lex, A. & Gehlenborg, N. UpSetR: an R package for the visualization of intersecting sets and their properties. *Bioinformatics* **33**, 2938–2940 (2017).
61. Hao, Y. *et al.* Integrated analysis of multimodal single-cell data. *Cell* **184**, 3573-3587.e29 (2021).
62. Yang, S. *et al.* Decontamination of ambient RNA in single-cell RNA-seq with DecontX. *Genome Biol.* **21**, 57 (2020).

Supplementary material

Supplementary Discussion

Supplementary Figures 1-3

Supplementary Tables 1-14